PHYSICAL REVIEW E VOLUME 59, NUMBER 4 APRIL 1999

Two-photon fluorescence imaging of impurity distributions in protein crystals

C. L. Caylor, I. Dobrianov, C. Kimmer, and R. E. Thorne*
Laboratory of Atomic and Solid State Physics, Cornell University, Ithaca, New York 14853

W. Zipfel and W. W. Webb
Department of Applied and Engineering Physics, Cornell University, Ithaca, New York 14853

(Received 20 November 1998)

Macromolecular impurities present in solution have profound effects on the growth and quality of protein crystals used for x-ray structure determinations. We have imaged the three-dimensional distribution of ovotransferrin impurities in crystals of the protein hen egg white lysozyme (HEWL) using two-photon excitation fluorescence microscopy. Impurity concentrations differ between the two types of growth sectors present in tetragonal HEWL crystals and impurities preferentially incorporate along the boundaries between growth sectors. Cracked crystals show large impurity-rich cores that are not observed in uncracked crystals. These nonuniform impurity distributions provide insight into how and why impurities affect crystal quality. Our results have implications for crystal growth and for protein purification. [S1063-651X(99)50804-0]

PACS number(s): 87.14.Ee, 87.15.Nn, 87.64.Vv, 61.72.Ss

The revolution occurring in molecular biology is being fueled in part by the growing availability of high-resolution structures of proteins and other biological macromolecules. These structures, most of which are determined by performing x-ray diffraction measurements on crystallized molecules, allow detailed insight into molecular function and the rational design of drugs to modify this function. To date, the structures of only $\sim 1\%$ of the proteins in the human body have been determined. Even with advances in x-ray sources, data collection methods, analysis tools, and molecular expression systems, the rate at which structures are being solved is still far behind the rate at which new molecules are becoming available for study. The most serious obstacle to more rapid structure determinations is now the difficulty of obtaining high-quality macromolecular crystals [1].

Of the many factors contributing to this difficulty, growth solution purity is among the most important. Compared with growth solutions used to prepare inorganic crystals, those used for growth of protein crystals tend to be extremely impure [2]. Total solution concentrations of impurity proteins may be up to several percent, and even high-purity commercial lysozymes—easily crystallized and widely used for fundamental growth studies—have impurity concentrations of at least one percent. Protein crystal impurities are much more diverse than those of inorganic crystals, and include structurally unrelated molecules that remain after purification, structurally related genetic variants of the host molecule, variants produced by post-translational modifications such as deglycosylation and deamidation, chemically identical conformational variants, and oligomers [3–7]. These impurities can have profound effects on solubility, nucleation, growth kinetics, and crystal habit and morphology, and can promote the creation of dislocations, cracks, and other disorder that can significantly degrade diffraction properties [3–15].

We have directly imaged the three-dimensional distribution of impurity molecules in lysozyme crystals using two-photon excitation fluorescence microscopy. Impurities are distributed nonuniformly in characteristic ways, and these nonuniformities produce the lattice stresses responsible for dislocation formation and crystal cracking. These insights suggest an approach for obtaining high-quality crystals from heavily contaminated growth solutions and have implications for the use of crystallization in protein purification.

Tetragonal hen egg white lysozyme (HEWL) crystals were grown from supersaturated solutions containing 20–30 mg/ml high-purity commercial lysozyme (Seikagaku) and 0.75 M NaCl dissolved together with fluorescently labeled impurities in 0.1 M acetate buffer at pH 4.5. 10 μl drops of this solution were suspended on siliconized cover slips in sealed wells over solutions with the same buffer and salt concentrations and then maintained at a constant temperature for several days until crystals appeared. Our initial focus has been on ovotransferrin (Sigma), a structurally unrelated protein whose molecular weight (78 kDa) is roughly five times that of lysozyme (14.6 kDa) and which is sometimes present as an impurity protein in commercial lysozyme [4–7]. Fluorescently labeled ovotransferrin was prepared using the Alexa 488 Protein Labeling Kit (Molecular Probes). The molecular weight of the attached label, $\sim$520 Daltons, is much smaller than that of ovotransferrin. Absorbance measurements indicate that an average of 3 to 4 labels attach to each molecule. Attached labels will in general modify the incorporation behavior, so that labeled ovotransferrin is best considered as a distinct impurity from its unlabeled form. Most growth experiments used solution concentrations of 0.5% w/w labeled ovotransferrin and yielded crystals that were well-faceted but often visibly cracked.

Two-photon excitation fluorescence microscopy measurements were performed using the facilities of the Developmental Resource for Biophysical Imaging and Optoelectronics (DRBIO) at Cornell. In this technique, a femtosecond infrared laser beam focused through the objective lens of a microscope excites fluorescence by a two-photon absorption process [16]. The laser is raster scanned across the sample and the non-descanned epifluorescence is collected by a pho-

*Electronic address: ret6@cornell.edu

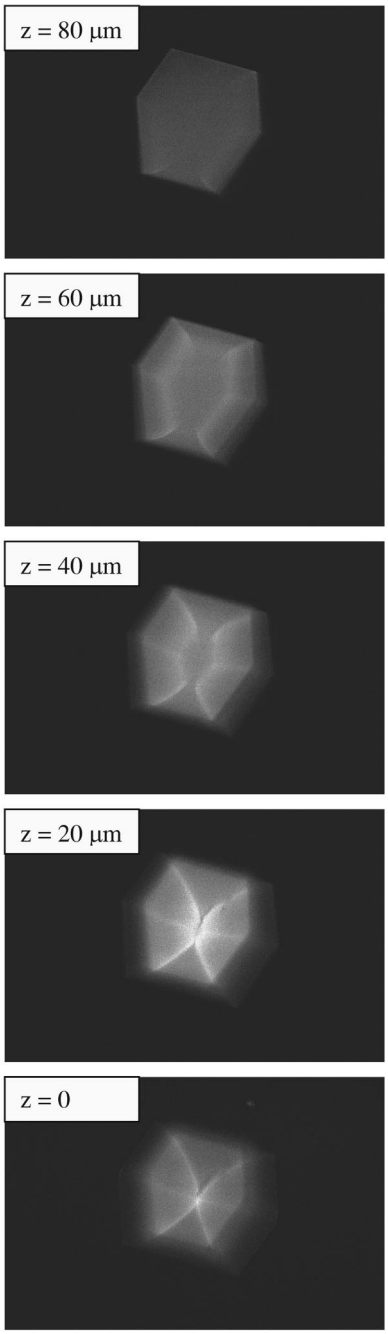

FIG. 1. Two-photon fluorescence micrographs of an uncracked lysozyme crystal grown from a solution containing ~0.5% labeled ovotransferrin, acquired at successive heights z from the initial crystal nucleus at $z=0$. Image widths are 700 μm.

tomultiplier tube and integrated for the pixel dwell time (~1.5 ms) to form a digital image of a two-dimensional plane in the crystal. Images of successive planes are obtained by stepping the objective focus vertically relative to the sample. Pixel intensities are proportional to the local concentration of fluorophores, so an absolute measure of the incorporated impurity density can be obtained after calibration using a sample containing a known concentration of labeled ovotransferrin.

Conventional (one-photon) fluorescence microscopy has very recently been used to image labeled avidin impurities in HEWL crystals and to show that impurity incorporation depends upon growth rate [17]. For two-photon excitation, the fluorescence is proportional to the intensity squared rather than the first power of intensity. As a result, the excitation volume at the focus is much more precisely defined both laterally and vertically, and attenuation of the incident beam as it passes through the crystal is dramatically reduced, simplifying interpretation of results. For the objective lens used in these experiments, the lateral and axial widths of the two-photon excitation volume (uncorrected for crystal geometry and interface refraction effects) are ~0.4 and ~5.3 μm, respectively. The limiting factors on the resolution of the images are then (laterally) the pixel width of ~1.8 μm and (vertically) the chosen step size of 10 μm between consecutive images. This high spatial resolution allows true three-dimensional imaging and observation of features that are not visible by conventional fluorescence microscopy.

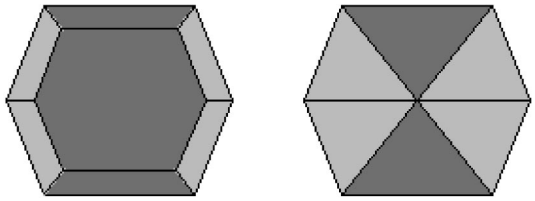

FIG. 2. Growth sector structure of tetragonal lysozyme crystals in slices parallel to a (110) face, taken (a) through the center of the crystal and (b) away from the center. The dark gray regions are (110) sectors, and the light gray regions are (101) sectors.

Figure 1 shows a series of two-photon fluorescence micrographs of an uncracked crystal taken at successive vertical positions z, where $z=0$ corresponds to the approximate position of the initial crystal nucleus and the z-axis in this case is oriented along a [110] direction. The observed fluorescence indicates that impurities incorporate in the crystal, and a calibration yields an impurity segregation coefficient of ~0.4. Figure 2 illustrates the expected growth sector structure for slices perpendicular to the (110) direction; the dark gray regions correspond to (110) growth sectors [formed by addition of molecules to the (110) faces], and the light gray regions correspond to (101) growth sectors. Comparison with Fig. 1 reveals two interesting features. First, the fluorescence intensity and thus the incorporated impurity density is different in the (110) and (101) growth sectors; measurements on several crystals indicate $I(110)/I(101)\sim 0.5$–0.8. Second, the boundaries between growth sectors—particularly between inequivalent growth sectors—are brighter than nearby regions by as much as a factor of 1.5, implying that impurities preferentially incorporate there. The curvature of the sector boundaries in Fig. 1 results from variations in the relative face growth rates as supersaturation declines during growth [12].

Figure 3 shows a similar series of images (with z along a [001] direction) for a cracked crystal grown under conditions nominally identical to those for the crystal in Fig. 1. In this case, the crystal shows fluorescence in its core that is much more intense than in later growth regions, which have intensities comparable to those of uncracked crystals. The observed intensities imply that the core impurity concentration is at least a factor of six larger than the bulk concentration and that the diameter of the core is roughly 50 μm. Large impurity-rich cores have been observed in all cracked crys-

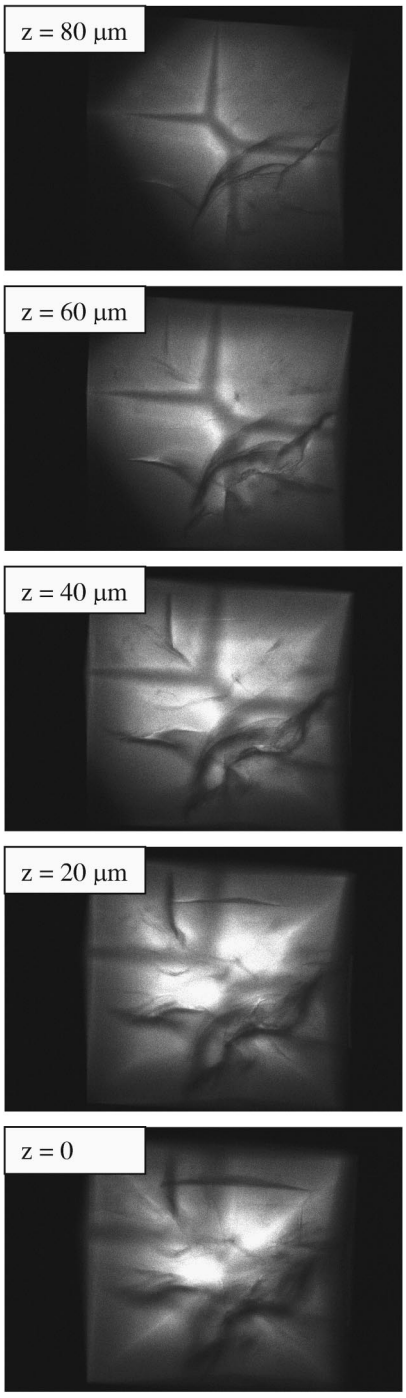

FIG. 3. Two-photon fluorescence micrographs of a cracked lysozyme crystal grown from a solution containing ~0.5% labeled ovotransferrin. Image widths are 700 μm.

tals studied but have not been observed in uncracked crystals [18]. Vekilov *et al.* [19] found that average incorporated salt and impurity concentrations in lysozyme crystals decreased with increasing crystallized fraction and thus increasing average crystal size. Based on analysis of salt incorporation and the correlation between salt and impurities, they concluded that lysozyme crystals have a salt and impurity-rich core roughly 40 μm in diameter. The data of Fig. 3 provide direct evidence for impurity-rich cores.

The observation of nonuniform impurity distributions in HEWL crystals gives insight into how impurities create disorder. As is well established in inorganic crystal growth, impurity incorporation changes crystal lattice constants, and nonuniform incorporation creates stresses [20]. Sectorial differences in impurity incorporation create stresses along growth sector boundaries that can drive formation of dislocations and cracks. Assuming that the molecular volume in the lattice scales with molecular weight, the measured ovotransferrin densities in the (101) and (110) growth sectors imply a lattice constant difference between sectors of ~0.1%. This difference is substantial and must produce significant disorder along the growth sector boundaries. Decoration of these boundaries by impurities suggests that the disorder facilitates impurity incorporation. However, since both cracked and uncracked crystals display significant sectorial inequalities, the associated stresses do not seem to be the dominant source for the cracking observed in our experiments.

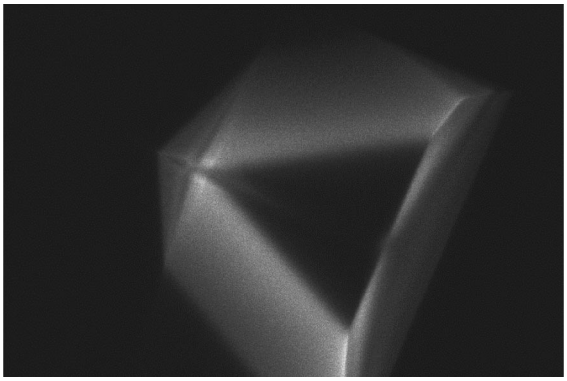

FIG. 4. Two-photon fluorescence micrograph of a lysozyme crystal grown from a pure seed in a solution containing ~0.5% labeled ovotransferrin and ~4.5% unlabeled ovotransferrin. Image widths are 700 μm.

Radial impurity concentration variations can result if incorporation on a given growth face varies in time. Crystal growth causes growth solution depletion and enrichment of its various components and changes in concentration and flow profiles, and these in general affect impurity incorporation. For example, solution supersaturation usually decreases as growth proceeds, and the higher growth rates that occur immediately after nucleation can bury impurities before they have time to desorb [20]. This could account for the impurity rich cores observed in cracked crystals. Some crystals grown under nominally identical conditions (e.g., Fig. 1) do not show impurity rich cores, but these may nucleate later and at a lower supersaturation.

Enhancement of the impurity density in the crystal core may also result if the initial nucleus has a high defect density, perhaps because of impurity effects on initial aggregation. As happens at growth sector boundaries, impurities may decorate these defects, increasing the total impurity concentration. However, the defect density required to account for the observed core impurity density is very high.

If impurities create cracks and other relevant disorder primarily via their incorporation behavior in the early stages of growth, then one might hope to grow well-ordered crystals from highly impure solutions by using a pure seed. To test this idea, crystals were nucleated in pure lysozyme solutions and then transferred to solutions containing 0.5% w/w la-

beled ovotransferrin and 4.5% unlabeled ovotransferrin for further growth [21]. Crystals that spontaneously nucleate in such solutions invariably crack and show other evidence of disorder. However, as indicated by the fluorescence micrograph of Fig. 4, crystals grown from pure seeds in such solutions are generally free of visible defects. In the growth region outside the seed, the absolute labeled ovotransferrin concentration and the sectorial concentration differences are comparable to the bulk results for unseeded crystals. This provides additional evidence that bulk incorporation is not responsible for the defects observed in unseeded crystals.

Finally, we note that the present results may have implications for protein purification by crystallization. In typical commercial crystallization, the supersaturation is greatly and rapidly increased, producing a shower of small, often heavily defected crystals. If impurities are preferentially incorporated in crystal cores and decorate crystal defects, then substantial impurity densities may remain in the crystallized fraction. This may explain why impurities that growth studies find do not appreciably incorporate in the crystal bulk often heavily contaminate commercial recrystallized lysozyme. By growing larger crystals using more gradual supersaturation changes, greater separation efficiency should be obtained.

We wish to thank A. A. Chernov, G. DeTitta, S. Ealick, S. Kriminski, B. R. Thomas, and W. W. Webb for fruitful discussions. This work was supported by NASA (Grant No. NAG8- 1357). C.C. and C.K. acknowledge support provided by the National Science Foundation and the U.S. Department of Education, respectively. W.Z. and the DRBIO were supported by the NIH (Grant No. P412RR04224) and the NSF (Grant No. BIR/DB1-9419978).

[1] For example, see N. E. Chayen, T. J. Boggon, A. Cassetta, A. Deacon, T. Gleichmann, J. Habash, S. J. Harrop, J. R. Helliwell, Y. P. Nieh, M. R. Peterson, J. Raftery, E. H. Snell, A. Hadener, A. C. Niemann, D. P. Siddons, V. Stojanoff, A. W. Thompson, T. Ursby, and M. Wulff, Q. Rev. Biophys. **29**, 227 (1996).

[2] A. McPherson, *Preparation and Analysis of Protein Crystals* (Krieger, Malabar, FL, 1982); in *Crystallization of Nucleic Acids and Proteins*, edited by A. Ducruix and R. Giege (IRL, Oxford, 1992).

[3] L. J. Wilson and F. L. Suddath, J. Cryst. Growth **116**, 414 (1992).

[4] B. Lorber, M. Skouri, J.-P. Munch, and R. Giege, J. Cryst. Growth **128**, 1203 (1993).

[5] M. Skouri *et al.*, J. Cryst. Growth **152**, 209 (1995).

[6] F. L. Ewing, E. L. Forsythe, M. van der Woerd, and M. L. Pusey, J. Cryst. Growth **160**, 389 (1996).

[7] B. R. Thomas, P. G. Vekilov, and F. Rosenberger, Acta Crystallogr., Sect. D: Biol. Crystallogr. **52**, 776 (1996).

[8] C. Abergel, M. P. Nesa, and J. C. Fontecilla-Camps, J. Cryst. Growth **110**, 11 (1991).

[9] E. Forsythe, F. Ewing, and M. L. Pusey, Acta Crystallogr., Sect. D: Biol. Crystallogr. **50**, 614 (1994).

[10] E. Forsythe and M. L. Pusey, J. Cryst. Growth **139**, 89 (1994).

[11] K. Provost and M. C. Robert, J. Cryst. Growth **156**, 112 (1995).

[12] P. G. Vekilov, L. A. Monaco, and F. Rosenberger, J. Cryst. Growth **156**, 267 (1995).

[13] J. Hirschler and J. C. Fontecilla-Camps, Acta Crystallogr., Sect. D: Biol. Crystallogr. **52**, 806 (1996).

[14] P. G. Vekilov and F. Rosenberger, J. Cryst. Growth **158**, 540 (1996).

[15] J. Hirschler, F. Halgand, E. Forest, and J. C. Fontecilla-Camps, Protein Sci. **7**, 185 (1998).

[16] W. Denk, J. H. Strickler, and W. W. Webb, Science **248**, 73 (1990); C. Xu *et al.*, Proc. Natl. Acad. Sci. USA **93**, 10 763 (1996).

[17] K. Kurihara, S. Miyashita, G. Sazaki, T. Nakada, H. Komatsu, T. Ohba, and K. Ohki, J. Cryst. Growth **196**, 285 (1999).

[18] Uncracked crystals (as in Fig. 1) do have some modest impurity enrichment in their cores because impurities decorate growth sector boundaries, and the ratio of sector suface area to volume diverges in the core.

[19] P. G. Vekilov, L. A. Monaco, B. R. Thomas, V. Stojanoff, and F. Rosenberger, Acta Crystallogr., Sect. D: Biol. Crystallogr. **52**, 785 (1996).

[20] A. A. Chernov, *Modern Crystallography II. Crystal Growth* (Springer, Berlin, 1984).

[21] Additional unlabeled ovotransferrin was included in the new growth solution to reduce the rate of spontaneous nucleation—making it easier to visually distinguish the transferred crystal—and to allow post-transfer growth in a medium impure by protein crystal growth standards (5% w/w).